

Neutron capture processes

elements \rightarrow Fe not effectively produced

by reactions between charged particles

instead: n-capture on seed nucleus

(mostly ^{56}Fe)

- s-process following the stability valley
- r-process SN II outburst or other high-energy events related to n-stars

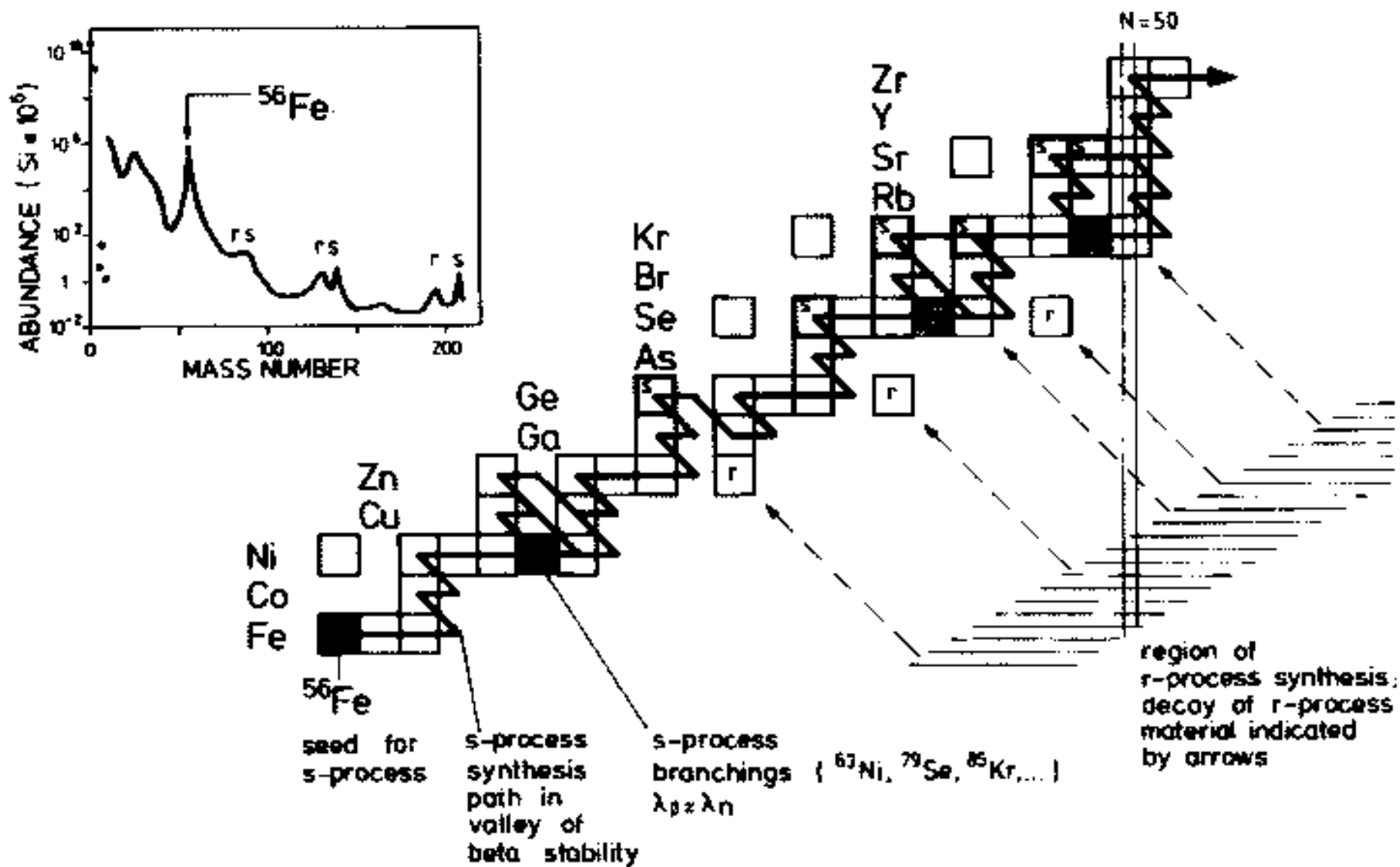


Fig. 6.1. Part of the s-process path, showing some s-only nuclei (marked 's') and some branchings between n -capture and β^- -decay (shaded boxes), which give an idea of relevant neutron densities and temperatures. After Käppeler, Beer and Wissak (1989). Copyright by IOP Publishing Ltd. Courtesy Franz Käppeler.

S-process

where does this happen?

branchings between n-capture & β^- decay

$$(t_{1/2})^{-1} \sim \sigma \phi$$

$t_{1/2}$ β -decay half life
time

σ n-capture cross sect.

ϕ n-flux $\phi = u_n \langle v \rangle$

typical $T \sim 10^8 K$ (He burning) $\rightarrow \langle v \rangle \sim 10^8 \frac{cm}{s}$

$$\sigma \sim 100 mb \quad t_{1/2} = 300 a$$

$$\Rightarrow u_n \sim 10^7 cm^{-3}$$

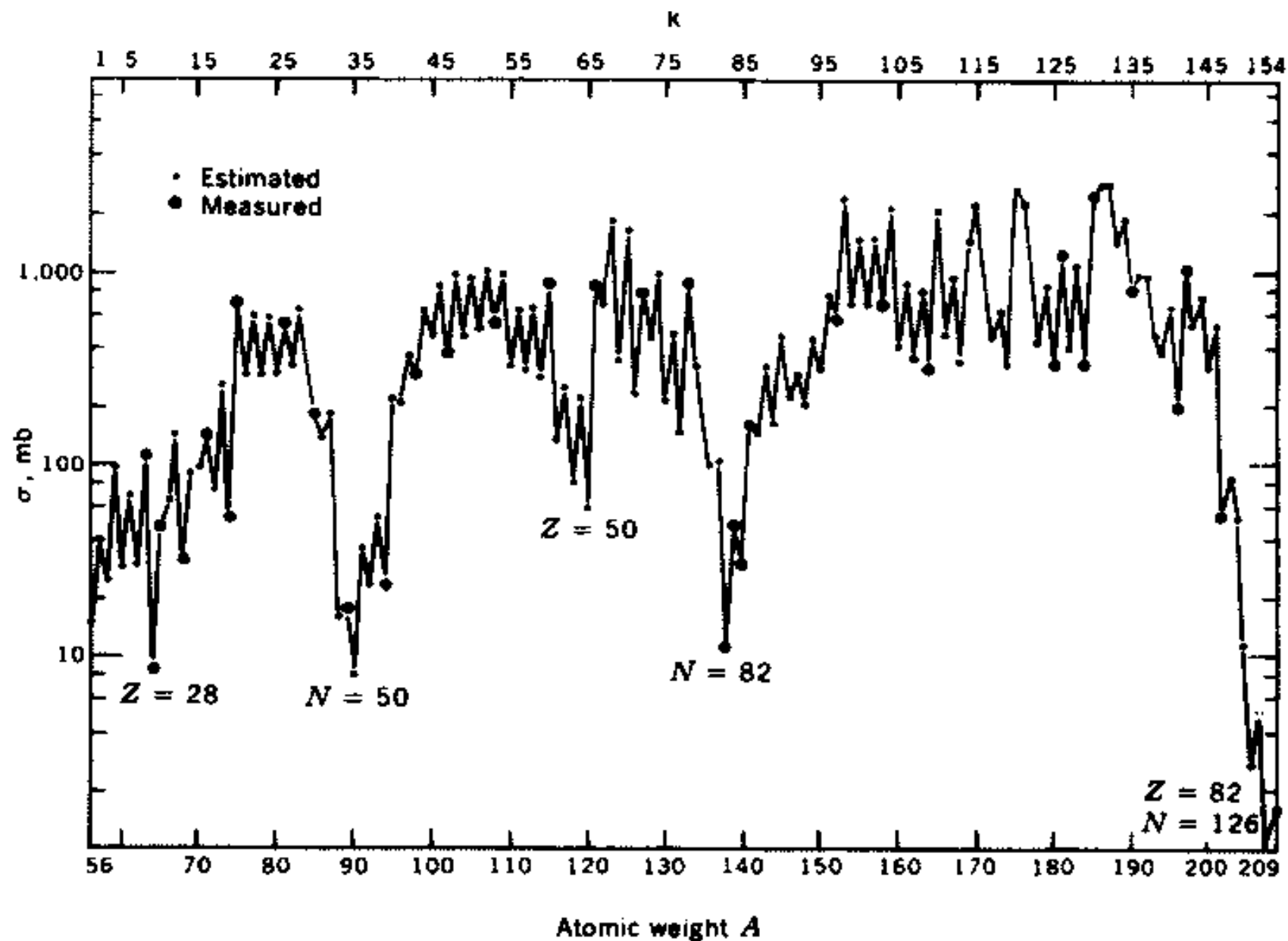


Fig. 6.2. Neutron-capture cross-sections at energies near 25 keV. Very large dips occur at the magic numbers. After Clayton (1984). Copyright by the University of Chicago. Courtesy Don Clayton.

more detailed considerations:

$$\bar{T} \sim 4 \cdot 10^8 \text{ K} \quad n_n \sim 10^8 \text{ cm}^{-3}$$

total mass density 2500 to 13 000 g/cm³

typical for He-shell burning zones

analytical theory of s-process

simple chain starting with ⁵⁶Fe as seed

neutron irradiation or fluence

$$\bar{\tau} = \oint \phi dt = \int n_n \langle v \rangle dt$$

abundances are governed by

$$(1) \quad \frac{dN_i}{d\tau} = \sigma_{i-1} N_{i-1} - \sigma_i N_i \quad 56 \leq i \leq 209$$

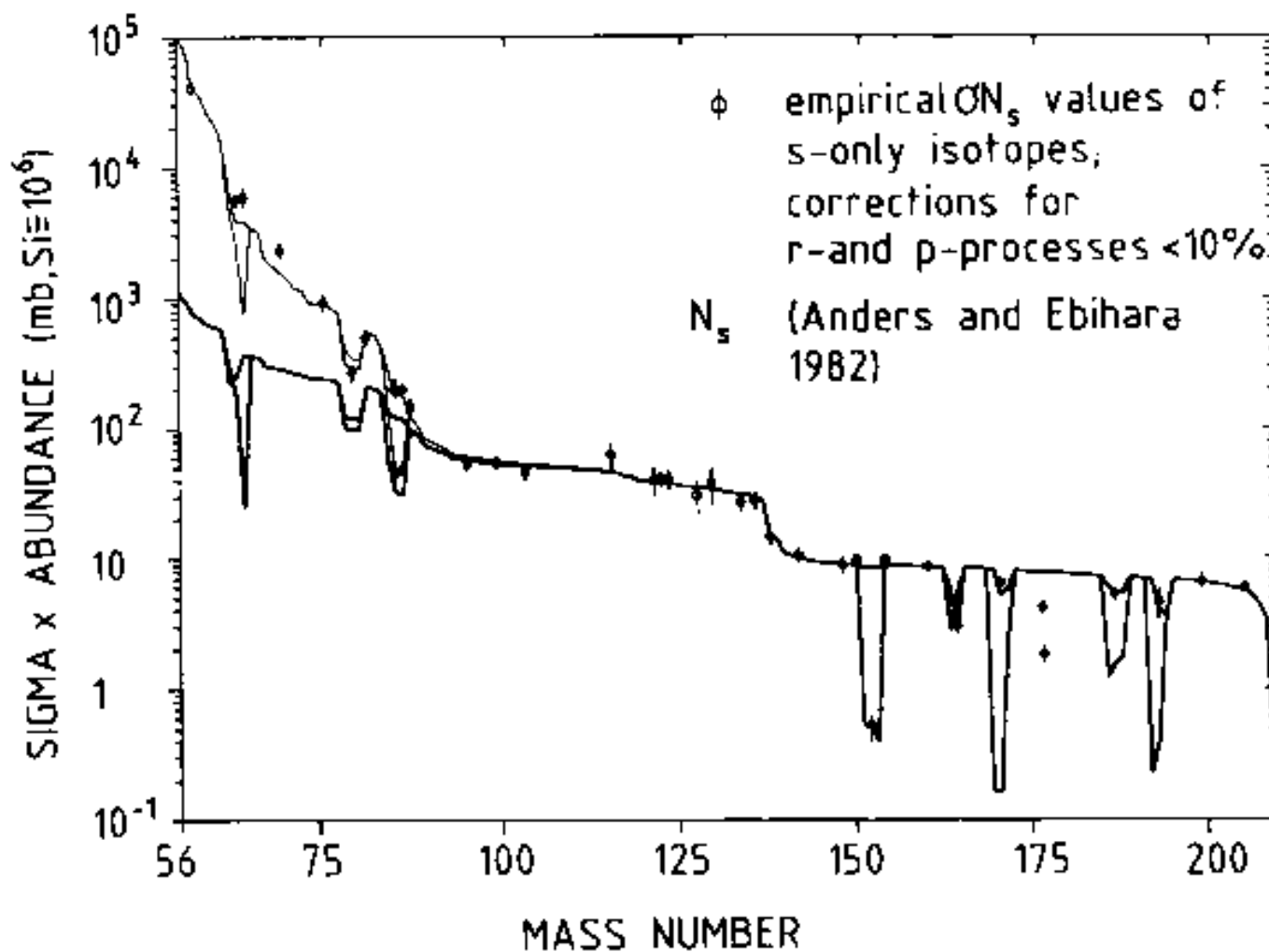


Fig. 6.3. Product σN of abundance and neutron capture cross-section for s-only nuclides in the Solar System. The main and weak s-process components are shown by the heavy and light curves respectively. Units are mb per 10^6 Si atoms. After Käppeler, Beer and Wisshak (1989). Copyright by IOP Publishing Ltd. Courtesy Franz Käppeler.

initial conditions $N_{56}(0) = 1$ $N_{i \neq 56}(0) = 0$

in steady state $\frac{dN_i}{dt} = 0$

$\sigma N = \text{const.}$ (breaks down close to magic numbers)

general solution of (1)

$$N_k(\tau) = \sum_{i=56}^k C_{ki} e^{-\sigma_i \tau}$$

$$\text{where } C_{56,56} = 1 \quad C_{57,56} = -C_{56,57} = \frac{\sigma_{56}}{\sigma_{57} - \sigma_{56}}$$

$$C_{ki} = \prod_{j=56}^k \left(\frac{\sigma_j}{\sigma_j - \sigma_i} \right); \quad j \neq i$$

problem: small inaccuracies in $\sigma_j - \sigma_i$ lead to large errors

→ use approximation, based on exponential distribution

$$p(\tau) d\tau = e^{-\tau/\tau_0} \frac{d\tau}{\tau_0}$$

→ abundances given by

$$(2) \quad \tilde{N}(\tau_0) = \int_0^{\infty} N(\tau) p(\tau) d\tau$$

(Laplace transform of the solution for single fluence)

$$\Rightarrow \int_0^{\infty} \frac{dN_{56}}{d\tau} e^{-\tau/\tau_0} \frac{d\tau}{\tau_0} = -\tau_0 \tilde{N}_{56}(\tau_0)$$

$$\text{integrating: } \tilde{N}_{56}(\tau_0) - 1 = -\tau_0 \tilde{N}_{56}(\tau_0)$$

$$\text{similarly } \frac{1}{\tau_0} \tilde{N}_{57}(\tau_0) = -\sigma_{57} \tilde{N}_{57}(\tau_0) + \sigma_{56} \tilde{N}_{56}(\tau_0)$$

→ series of algebraic equations

$$\sigma_{56} N_{56} = \frac{1}{\tau_0} \left(1 + \frac{1}{\tau_0 \sigma_{56}} \right)^{-1}$$

$$\sigma_{57} N_{57} = \frac{1}{\tau_0} \left(1 + \frac{1}{\tau_0 \sigma_{56}} \right)^{-1} \left(1 + \frac{1}{\tau_0 \sigma_{57}} \right)^{-1}$$

$$\sigma_k N_k = \frac{1}{\tau_0} \prod_{i=56}^k \left(1 + \frac{1}{\tau_0 \sigma_i} \right)^{-1}$$

can be solved from top to down

as $\tau_0 \sigma_i$ is large: σN declines slowly with atomic mass number k

when σ becomes small at magic numbers:
sudden drop

(2) with $\tau_0 \sim 0.3 \text{ mb}^{-1}$ at $\bar{E} = 30 \text{ keV}$
gives excellent Solar-System abundances
above $A=80$ (Kr) to 90 (Zr)

exp-distribution is elegant, but reality
is more complicated

for low mass numbers an additional
weak component is required

single fluence $\tau \sim (4 \text{ mb})^{-1}$

or exp-distribution $\tau_0 = (16 \text{ mb})^{-1}$

He + C burning zones in massive stars

ratios $^{37}\text{Al}/^{36}\text{Ar}$ & $^{44}\text{K}/^{40}\text{Ca}$ indicate

< 1% of Solar-system material

has been s-processed

another parameter:

mean number of n captured by iron seed

$$n_c = \frac{\sum_{57}^{209} (A-56) N(A)}{N(56)} = \frac{1}{\tau_0} \sum_{57}^{209} \frac{A-56}{\sigma_A} \prod_{i=56}^A \left(1 + \frac{1}{\tau_0 \sigma_i}\right)^{-1}$$

$$\text{mean free time } \tau_0 \text{ (cm}^2/\text{sec})^{-1} \Rightarrow n_c \sim 10$$

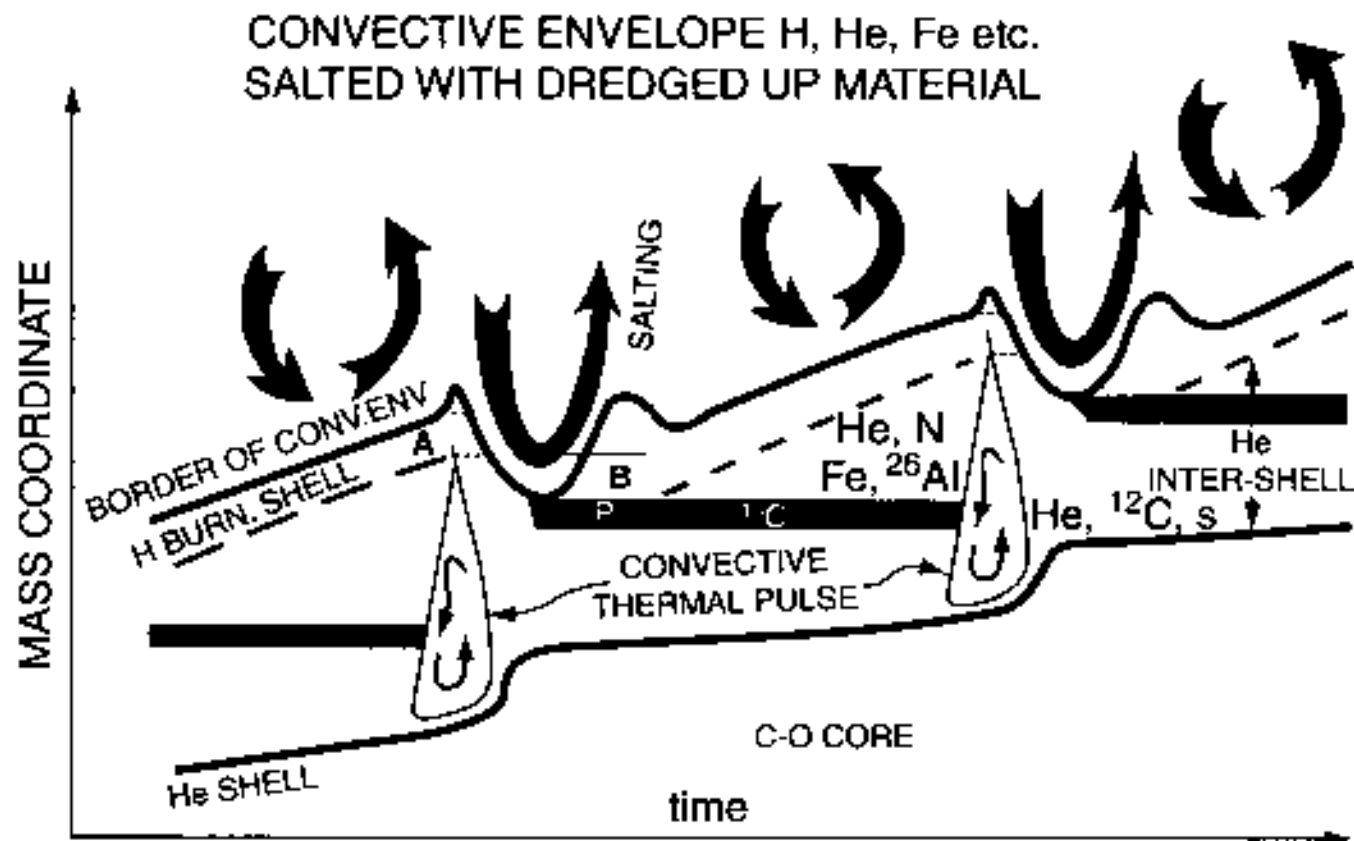


Fig. 6.4. Schematic view of ingestion during and after a thermal pulse in an AGB star. Pulses appear on an expanded scale owing to their short duration (~ 300 yr) compared to the inter-pulse period ($\sim 10^4$ to 10^5 yr). After Busso, Gallino and Wasserburg (1999). Reprinted with kind permission of Annual Reviews, Inc. Courtesy Maurizio Busso.

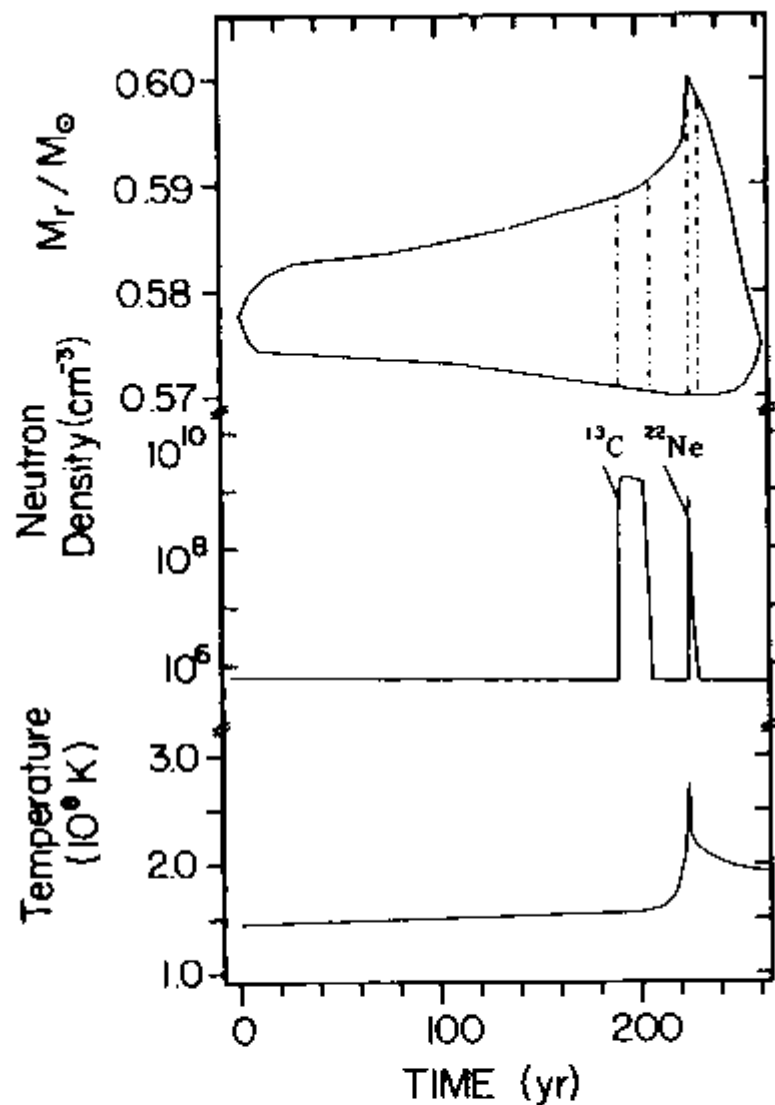
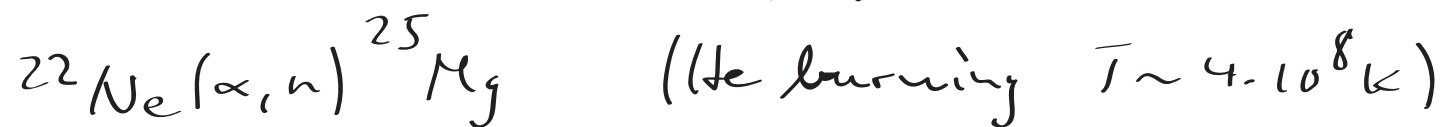


Fig. 6.5. Development of the convective region, neutron density from ^{13}C and ^{22}Ne sources and maximum temperature as functions of time during a thermal pulse in a low-mass star with $Z \simeq Z_\odot/3$, which seems to give the best fit to Solar-System abundances from the main s-process. However, more recent models imply that ^{13}C is all used up in the radiative phases. After Käppeler *et al.* (1990). Courtesy Maurizio Busso and Claudia Raiteri.

→ strong constraints on physical environment



does not contribute to main s-process
 n_c too low, n captured by Ne

main contribution through



exponential fluence distribution is a result
of successive thermal pulses in a star
in the asymptotic giant branch

during pulse: He core increases in mass

through H shell burning by ΔM_α

\rightarrow rise to fluence $\Delta \bar{\tau}$ of slow neutrons

material is mixed into inter-shell

convective region of mass M_{isc} generated
by the next puls

thus $\frac{M_\alpha}{M_{\text{isc}}} = 1 - r$ receives fluence $\Delta \bar{\tau}$
for first time

remaining fraction r overlaps with
previous pulse and has seen a fluence
of $2\Delta \bar{\tau}$

→ steady state is reached after several pulses

and probability of an exposure unit is

$$(1-r) r^{n-1} = \frac{1-r}{r} r^{\bar{\tau}/\tau} \propto e^{-\bar{\tau}/\bar{\tau}_0}$$

where $\bar{\tau}_0 = \Delta\tau / \ln(\frac{1}{r})$

$$\sim 10^{-6} \text{ to } 10^{-5} \text{ M}_\odot \text{ of } ^{13}\text{C}$$

Serve as n-source for s-process

r-process

needed to produce h-rich nuclei and
for species above ^{209}Bi .

in Solar System 27 r-only nuclides

it is presumably a coincidence that
s- and r-process have about the same level
in our Galaxy

physical environment for r-process

Fe seed nuclei need to capture many n's
leading to unstable nuclei with very short
 β -decay half lives, demanding high n-density

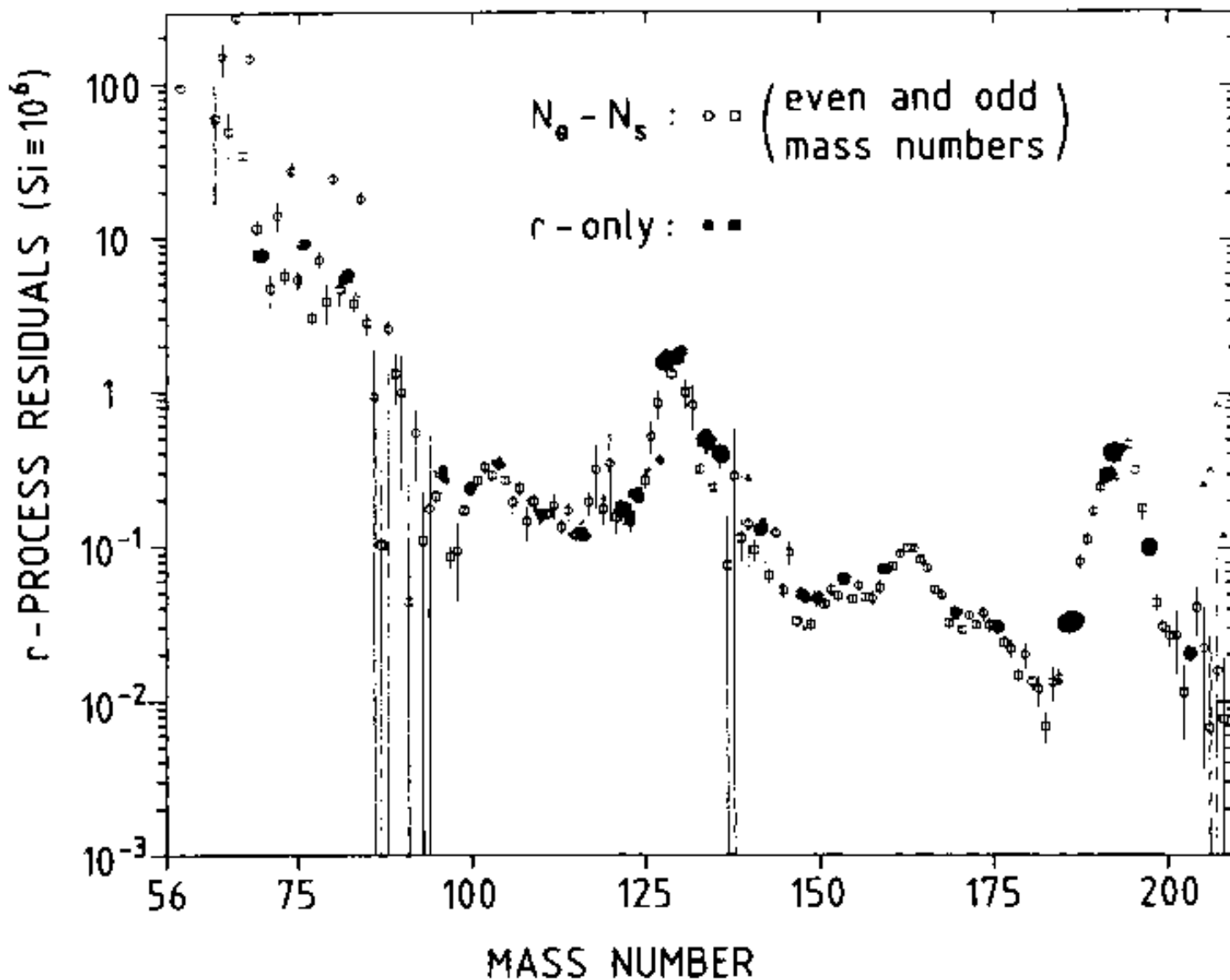


Fig. 6.7. r-process abundances in the Solar System. Filled circles represent r-only nuclides, while open circles with error bars show the result of subtraction of a calculated s-process contribution. After Käppeler, Beer and Wissak (1989). Copyright by IOP Publishing Ltd. Courtesy Franz Käppeler.

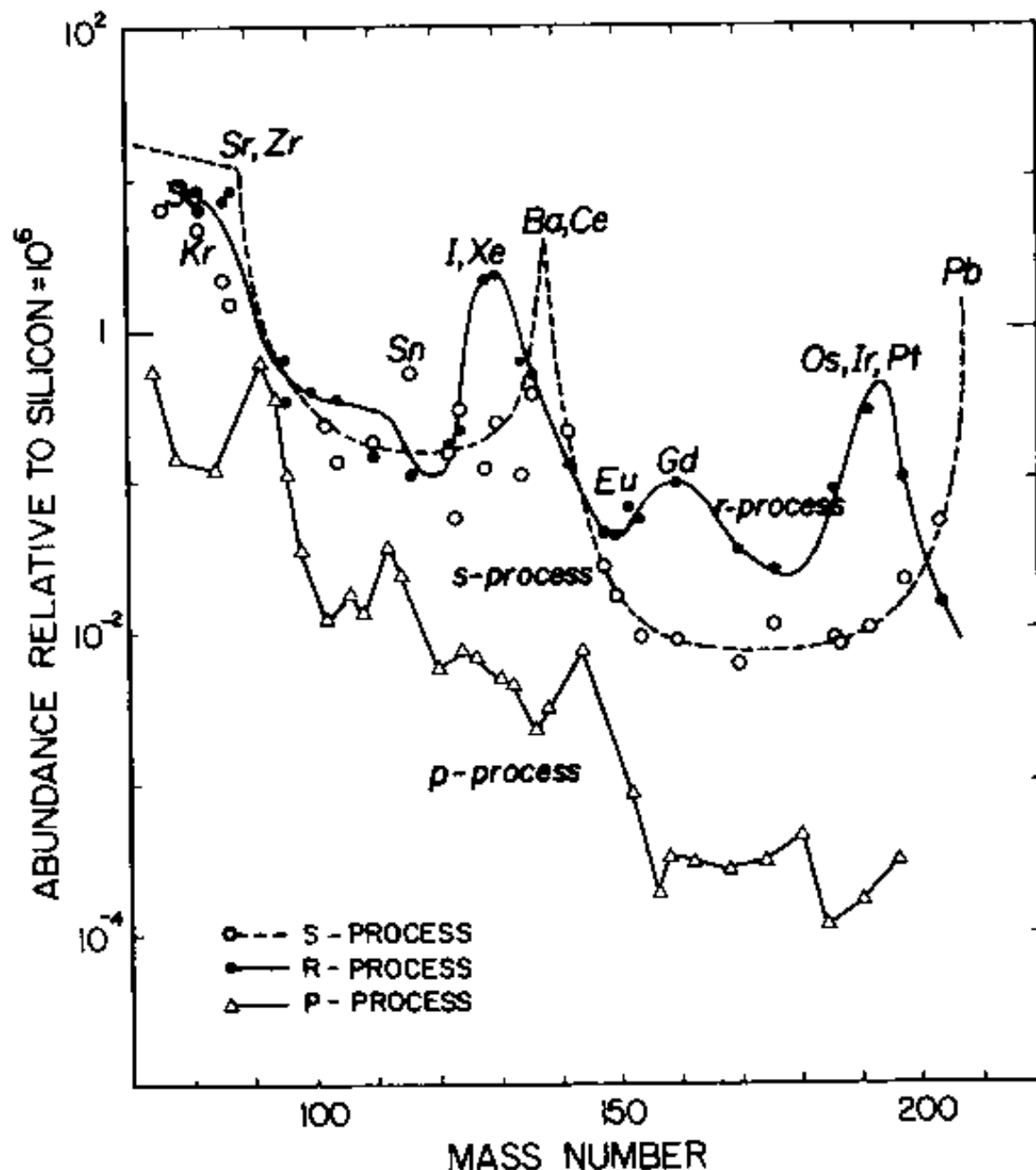


Fig. 6.8. Abundance curves for s-process (broken line), r- and p-process products (solid lines) in the Solar System. Adapted from Cameron (1982).

Table 6.3. *Relative r and s contributions to some elements in the Solar System*

Element	log N	s-weak	s-main	r
37 Rb	2.40	.14	.39	.47 ± .10
38 Sr	2.93	.09	.77	.14 ± .07
39 Y	2.22	.04	.85	.11 ± .06 :
40 Zr	2.61	.02	.78	.20 ± .03
56 Ba	2.21	.01	.88	.11 ± .02
57 La	1.20	.01	.75	.25 ± .08
58 Ce	1.61	.01	.77	.23 ± .01
59 Pr	0.71	.01	.45	.54 ± .09
60 Nd	1.47	.00	.46	.53 ± .03
62 Sm	0.97	.00	.30	.70 ± .03
63 Eu	0.54	.00	.03	.97 ± .06
66 Dy	1.15	.00	.12	.88 ± .15

Numbers in the first 4 rows (apart from the error estimates) are taken from Raiteri, Gallino and Busso (1992). The others are based on data for individual isotopes given by Käppeler, Beer and Wissak (1989).

$$t(n,\sigma) \ll t_\beta \approx 10^{-3} \text{ to } 1\text{s} \Rightarrow n_n > 10^{19} \text{ cm}^{-3}$$

such n-densities are probably associated with high T leading to reverse reactions (σ, n) reactions

for given τ , equilibrium of (n, σ) & (σ, n)

$$\frac{n(A+1, \tau)}{n(A, \tau)} \approx 10^{-34} n_n T_g^{-3/2} e^{Q/kT}$$

(Q: n separation energy)

increasing n_n drives abundance peak

where $N(A+1, \tau) = N(A, \tau)$ towards lower Q

$$Q = 2 \text{ MeV} \quad T = 10^9 \text{ K} \quad n_n = 10^{24} \text{ cm}^{-3}$$

used to calculate path (6.9)

at magic numbers:

each n-capture is followed by a β decay

\rightarrow zig-zag track

r-process path terminated by fission

near $A_{\max} = 270$ feeding matter back
at $A_{\max}/2$

followed by recycling as long n-supply lasts

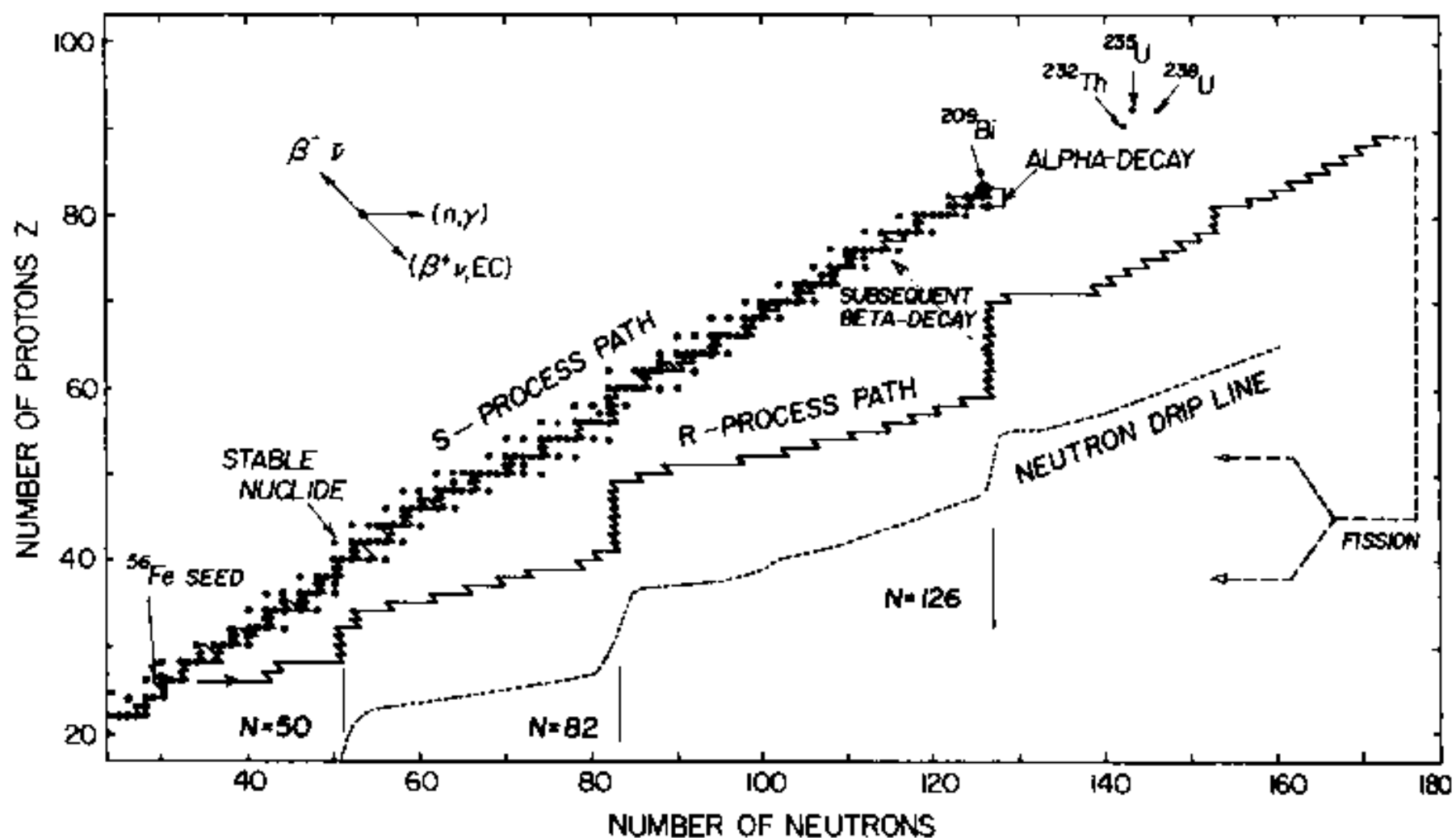


Fig. 6.9. Neutron capture paths in the N, Z plane. The r-process path was calculated for a temperature of 10^9 K and a neutron density of 10^{24} cm^{-3} (Seeger, Fowler & Clayton 1965). The dotted curve shows a possible location of the neutron drip line after Uno, Tachibana and Yamada (1992). Adapted from Rolfs and Rodney (1988).

→ number of heavy nuclei is doubled at each cycle

site of γ -process is not clear

it seems to take place in γ wind

surrounding a n-star in the early stage of a SN explosion

low-mass ($10 M_\odot$) S/N II

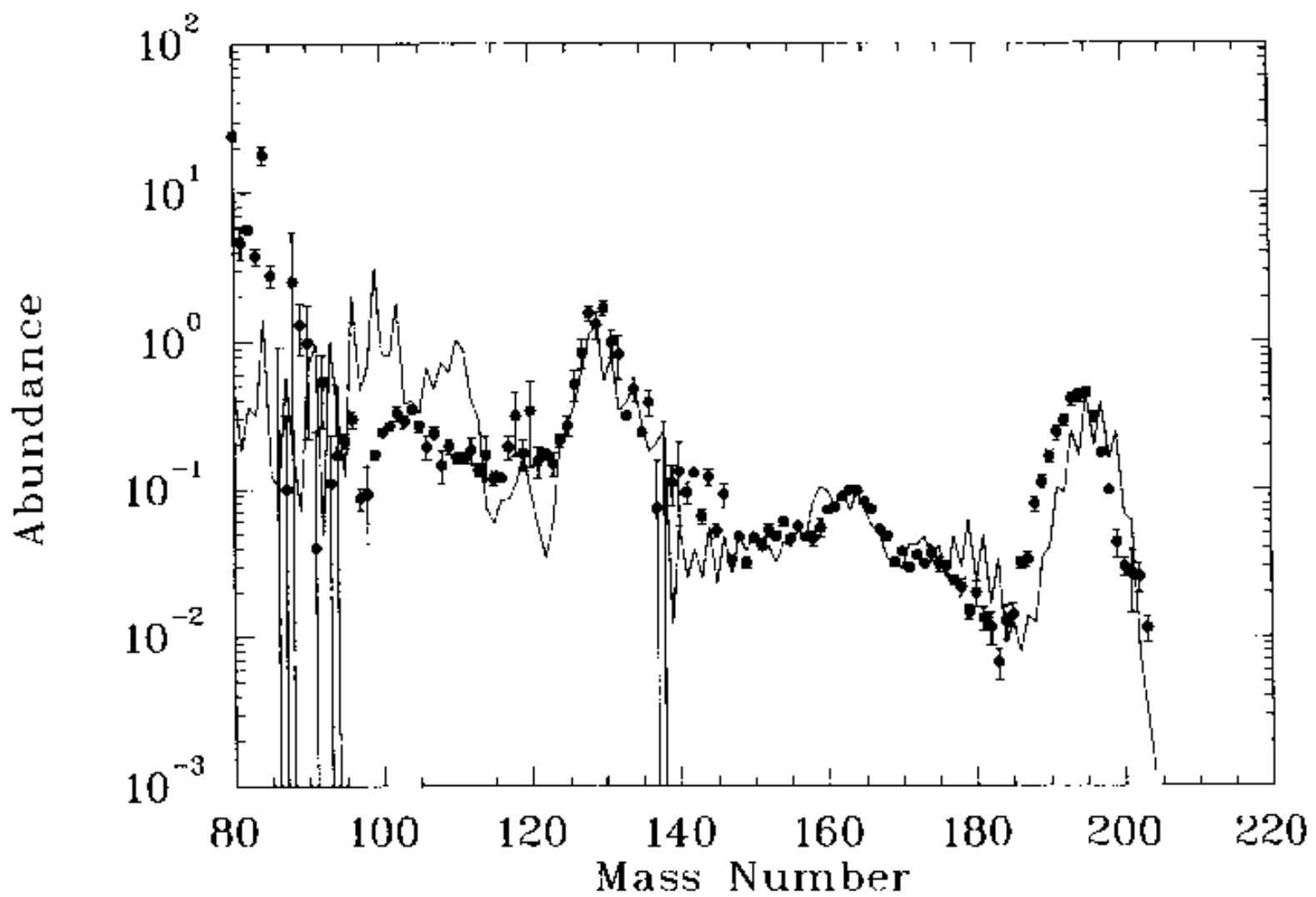


Fig. 6.10. Results of a dynamical calculation of the r-process in the hot neutrino bubble inside a $20 M_{\odot}$ supernova (continuous curve) compared to the observed Solar-System abundance distribution (filled circles). After Woosley *et al.* (1994). Courtesy Brad Meyer.